Chemistry SELECT

www.chemistryselect.org

A journal of ChemPubSoc Europe

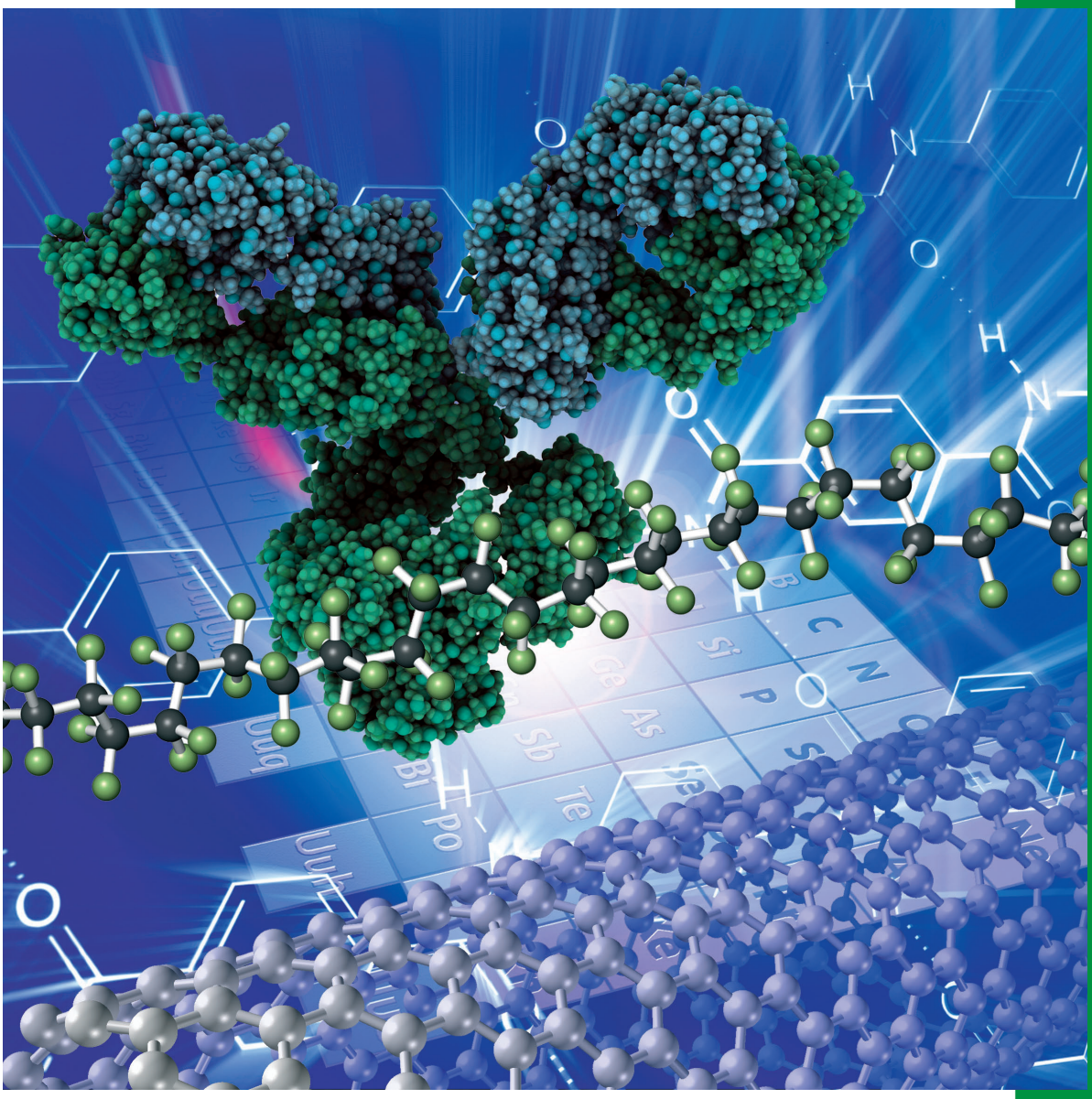

REPRINT

WILEY-VCH

ChemPubSoc Europe

DOI: 10.1002/slct.201701873

Chemistry SELECT Full Papers

Catalysis

One-Pot Synthesis of Tetrahydropyridine Derivatives: Liquid Salt Catalyst vs Glycolic Acid Promoter. Structure and Antiradical Activity of the New Products

Zorica D. Petrović,[a] Dušica Simijonović,[a] Jelena Đorović,[a, b] Vesna Milovanović,[a] Zoran Marković,[b, c] and Vladimir P. Petrović*[a]

Diethanolammonium hydrogensulfate (DHS), as a liquid salt, and glycolic acid (GA) were used for the synthesis of highly functionalized tetrahydropyridines (THPs). Due to the simplicity of the reaction procedure, excellent diastereoselectivity, and catalyst regeneration, these green protocols may be considered as an attractive approach for the preparation of THPs. Unlike numerous reported reactions for the synthesis of THPs that last for hours and with heating, GA-promoted reactions finished mostly within an hour and at room temperature. As improvement to other organocatalysed reactions for the synthesis of THPs with moderate yields, this protocol provided good to excellent yields. Application of these procedures produced three vanillic compounds reported here for the first time. Their structure was elucidated based on experimental and theoretical data (IR, ^{1}H NMR, ^{13}C NMR, NOESY, UV-Vis, and DFT). Experimental and theoretical antioxidant evaluation of these compounds has been carried out. DFT thermodynamical parameters supported experimental results that newly synthesized THPs deserve considerable attention as potent radical scavengers.

Introduction

Recently, multicomponent reactions (MCRs) have been recognized as very useful and efficient one-pot domino tool for the rapid formation of a wide range of different organic compounds.[1–5] Due to their properties such as atom economic, lower costs, and energy-saving, they have occupied a prominent place in the world of organic chemistry.[6] In the contrast to conventional multistep synthesis, these reactions provide instantaneous and elegant approach for the formation of new C–C and C–heteroatom bonds, as well as introduction of versatile functionalities. They often find application in the synthesis of structurally more or less complex biologically active N–heterocycles.

Some of piperidine core containing compounds are obtained using these reactions.[7,8] It is well known that these compounds exert numerous biological activities and that its structural motif is the part of many alkaloids and opiates. Morphine is probably the most famous representative of this class of compounds. Besides the analgesic effect of morphine,[9] they express cytotoxic activity,[10] they are commonly used as neuroleptics,[11] analeptics,[12] selective estrogen receptor modulators,[13] and many other activities.

Functionalized dehydropiperidines i.e. tetrahydropyridines, can be found in various natural alkaloids, biologically active synthetic molecules, and plentiful fine organic chemicals.[14,15] Many of them exert broad spectrum of pharmaceutical activities such as anti-hypertensive,[16] antibacterial,[17] antimalarial,[18] anticonvulsant,[19] anantihistaminic,[20] and anti-inflammatory.[21] For example, oligopeptide thiostrepton exerts multiple bioactivities. Apart from its antibiotic properties, thiostrepton exhibits antimalarial activity, as well as selective cytotoxicity against cancer cells.[22] Over the last ten years, numerous piperidine-containing compounds have been included into preclinical and clinical trials.[23]

For the synthesis of these scaffolds, several conventional methods have been used: Aza Diels-Alder reaction and some of its modifications, intramolecular Michael reaction, intramolecular Mannich reaction, tandem cyclopropane ring opening/Conia-ene cyclizations, and aza-Prins-cyclization.[24–28] Most of these methods are associated with numerous limitations and disadvantages, such as tedious and long procedure, lower yields, and use of toxic and expensive reagents and solvents.

Generally, organocatalysis provides effective way towards green chemistry, and suitable alternative for replacement of toxic metal and other catalysts which are environmentally harmful. It is known that liquid salts or ionic liquids (ILs) have been introduced to the assortment of available green solvents and tested as catalyst in numerous organic transformations including Heck and Mannich reactions.[29–35] Bearing this in mind, in the present study we synthesized liquid salt diethanolammonium hydrogensulfate (DHS), and tested for its

[a] Prof. Z. D. Petrović, Dr. D. Simijonović, J. Đorović, V. Milovanović, Dr. V. P. Petrović
University of Kragujevac, Faculty of Science, Department of Chemistry
Radoja Domanovića 12, 34000 Kragujevac, Republic of Serbia
E-mail: vladachem@kg.ac.rs
[b] J. Đorović, Prof. Z. Marković
Bioengineering Research and Development Center
Prvoslava Stojanovića 6, Kragujevac, Republic of Serbia.
[c] Prof. Z. Marković
Department of Chemical-Technological Sciences
State University of Novi Pazar
Vuka Karadžića bb, 36300 Novi Pazar, Republic of Serbia

Supporting information for this article is available on the WWW under https://doi.org/10.1002/slct.201701873

catalytic performance in THPs synthesis. Besides that, glycolic acid (GA) was used as promoter in new green protocol for the one-pot synthesis of these compounds. This acid, commonly present in fruit, exhibits multiple bioactivities, such as antioxidant activity and participation in biosynthesis of ceramide.[36] In addition, this compound is widely used in pharmacy and medicine, and its polymers are highly biodegradable compounds.[37–39] There are no results regarding any harmful effect to human health. To our best knowledge, there is no literature data regarding application of GA in MCRs, until now. In addition, results regarding antioxidant activity of phenolic THPs are missing. Bearing this in mind and the fact that antioxidants have very important role in prevention of diseases caused by free radical damage, these compounds deserve considerable attention.[40,41] The aim of this experimental and theoretical study is to structurally characterize newly obtained compounds, as well as to fulfil the gap of their antioxidant capacity.

Results and Discussion

Synthesis of THPs in MCRs

In the further course of catalytic application of ethanolamine based salts, DHS was synthesized, and its catalytic performance was inspected in one-pot MCR for the synthesis of THPs. Initially, model reaction of benzaldehyde, aniline and methyl acetoacetate was performed in ethanol, without addition of any catalyst, Table 1, Scheme 1. Formation of the product was

Table 1. Optimization of reaction conditions for the synthesis of highly functionalized THPs.

Entry	DHS/GA	time (h)	Temp.	Yield (%)	*anti:syn*
1	none	48	rt	/	/
2	none	48	reflux	/	/
3	DHS 10 mol%	24	rt	71	100:0
4	DHS 15 mol%	24	rt	77	100:0
5	DHS 20 mol%	24	rt	79	100:0
6	DHS 10 mol%	6	reflux	72	100:0
7	DHS 15 mol%	6	reflux	79	100:0
8	DHS 20 mol%	6	reflux	80	100:0
9	DHS 10 mol%	24	reflux	72	100:0
10	DHS 15 mol%	24	reflux	81	100:0
11	DHS 20 mol%	24	reflux	82	100:0
12	GA 20 mol%	24	rt	trace	/
13	GA 20 mol%	48	rt	trace	/
14	GA 20 mol%	6	reflux	50	75:25
15	GA 5%	4	rt	75	55:45
16	GA 5%	4	reflux	73	100:0
17	GA 30%	1	rt	92	100:0
18	GA 30%	1	reflux	93	100:0

not observed at room temperature, neither after heating of the reaction mixture to reflux for 48 h. In the presence of 10 mol% of the DHS catalyst, at room temperature for 24 h, the product was isolated in moderate yield. Increase of catalyst loading to up to 15 mol% improved reaction yields. Further increase of catalyst amount did not influence yield and reaction time significantly. On the other hand, heating of the reaction mixture

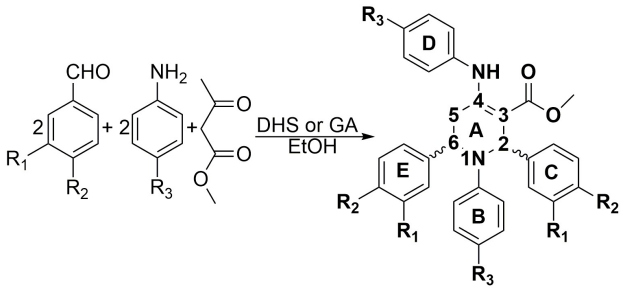

Scheme 1. General reaction for the synthesis of THPs.

to reflux in ethanol provided much shorter reaction time (6 h), without influence on reaction yield. Prolongation of the reaction time to up to 24 h, also did not have noteworthy influence. It is worth pointing out that only *anti* diastereoisomer was isolated (^{1}H NMR and NOESY).

In addition to catalytic performance of DHS, we tested GA for its behavior in this MCR. Catalytic amount of GA (20 mol%) provided formation of THP only in trace at room temperature, prolongation of reaction time to 48 h did not improve reaction yield, Table 1, entries 12 and 13, respectively. Larger amounts of this acid (5% GA solution in ethanol) at room temperature and under reflux provided much better results. In contrast to the reaction performed in the presence of catalytic amount of DHS, where only *anti*-product was isolated, here appearance of both diastereoisomers was observed. Namely, when lower amounts of GA were applied, *syn* isomers appeared in the reaction mixture, Table 1, entries 14 and 15. Finally, reaction with 30% of GA in ethanol at room temperature finished much faster (1 h), and with excellent yield (95%), giving exclusively *anti*-product. Increase of reaction temperature (reflux), did not influence yield and diastereoselectivity of this MCR. Based on the obtained result, optimal conditions in the case of DHS are 15 mol% of the catalyst and reflux in ethanol (**Method A**), while in the case of GA-assisted reaction, 30% GA solution in ethanol and at room temperature (**Method B**).

Optimal conditions for both methods were tested in the reactions with various aromatic aldehydes (4-chlorobenzaldehyde, 4-fluorobenzaldehyde and vanillin), anilines (aniline, 4-chloroaniline, and 4-methylaniline) and methyl acetoacetate, Tables 2 and 3. **Method A** produced exclusively *anti* diastereoisomer in good yields for all cases (about 75%), Table 2. On the other hand, yields of **Method B** reactions were even better (81–95%), but some of them did not produce exclusively *anti*-product, Table 3, entries **5**, **8**, and **11**. However, when these reactions were performed under reflux, diastereoselectivity of all **Method B** reactions was exclusively *anti*. It should be noted that vanillin-tetrahydropyridine products **1–3** are newly synthesized compounds. In addition, all THPs were isolated without using organic solvents, column chromatography, but only by washing of the precipitate with water and ethanol. Unlike the reactions with other aldehydes, those performed with vanillin lasted about 20 h. Reaction of 4-methylaniline, vanillin, and methyl acetoacetate proceeded in low yields. (Tables 2 and 3,

Table 2. Synthesis of THPs using **Method A**

entry	R_1	R_2	R_3	Yield[a] (%)	*anti*:*syn*[b] (%)
1	OCH_3	OH	H	75	100:0
2	OCH_3	OH	Cl	73	100:0
3	OCH_3	OH	CH_3	40	100:0
4	H	H	H	79	100:0
5	H	H	Cl	78	100:0
6	H	H	CH_3	79	100:0
7	H	F	H	75	100:0
8	H	F	Cl	73	100:0
9	H	F	CH_3	77	100:0
10	H	Cl	H	74	91:9
11	H	Cl	Cl	76	25:75
12	H	Cl	CH_3	78	91:9

[a]Reaction conditions: aldehyde (2 mmol), aniline (2 mmol), methylacetoacetate (1 mmol), and 15 mol% DHS, reflux in 1 ml of ethanol for 6 h; [b]Refers to diastereoisomeric ratios of room temperature reactions, which were determined from proton integration of *anti* and *syn* isomers from ^{1}H NMR spectra. Room temperature reactions lasted for 24 h. There was no significant difference in yields between corresponding reactions under reflux and room temperature reactions.

Table 3. Synthesis of THPs using **Method B**

entry	R_1	R_2	R_3	Yield[a] (%)	anti:syn[b] (%)
1	OCH_3	OH	H	88	100:0
2	OCH_3	OH	Cl	86	100:0
3	OCH_3	OH	CH_3	20	100:0
4	H	H	H	95	100:0
5	H	H	Cl	90	60:40
6	H	H	CH_3	93	100:0
7	H	F	H	87	100:0
8	H	F	Cl	85	60:40
9	H	F	CH_3	89	100:0
10	H	Cl	H	84	100:0
11	H	Cl	Cl	81	60:40
12	H	Cl	CH_3	83	100:0

[a]Reaction conditions: aldehyde (2 mmol), aniline (2 mmol), methylacetoacetate (1 mmol), and 30% GA solution in ethanol at room temperature; [b]Refers to diastereoisomeric ratios of room temperature reactions, which were determined from proton integration of *anti* and *syn* isomers from ^{1}H NMR spectra. Reactions under reflux lasted for 1 h. There was no significant difference in yields between corresponding reactions under reflux and room temperature reactions.

entry 3). Furthermore, change of reaction mediums (acetonitrile, methanol, water, ethanol:water (6:4), methanol:-water (6:4)), and prolongation of the reaction time did not contribute to the increase of the yield of the desired product. We assume that low performance of these reactions might be contributed to the strong electron donating nature of substituents of both, aldehyde and aniline, which is causing slower reactions.

Appearance of both diastereoisomers in some of the reactions performed at room temperature with **Method B**, encouraged us to test **Method A** for its performance at room temperature, Table 2. This way conducted **Method A** produced *syn* isomers in the cases where *para*-chlorobenzaldehyde was used (entries **10–12** in Table 2). In entries **10** and **12**, where aniline and 4-methylaniline were used, *anti*-isomer was the major product (about 90%). On the other hand, electron accepting substitution of aniline with chlorine provided formation of *syn*-isomer in excess, entry **11**. Appearance of the *syn* isomer was observed in all cases where chlorine was situated on aniline, Table 3. Unlike the reactions performed with **Method A**, *anti* THPs diastereoisomers were obtained in 20% excess in all cases where *syn* isomer appeared.

Mukhopadhyay at. al showed that reactions catalyzed with picric acid at lower temperatures yielded *syn* isomers in some cases. Bearing this in mind, the behavior of reaction from entry **11** was tested in "cold" conditions (0–5 °C). This reaction was selected because it is the only case where both methods yielded *syn* isomer. Due to significantly longer reaction time of **Method A**, **Method B** was used. Under these reaction conditions, the yield of the product was decreased to 45%, and only *syn* isomer was detected (^{1}H NMR and NOESY).

Different impact on *anti/syn* ratios in reactions performed with **Methods A** and **B** might be attributed to lower pH of the reaction mixture of **Method B** (about 3.5 and 1.5, respectively), and/or different reaction mechanisms of these methods. All reactions under reflux exposed exclusively *anti* diastereoselectivity. Decrease of the reaction temperature provoked appearance of the *syn* isomers in the cases were electron donating substituents are present. Therefore, it can be considered that *anti*-product is thermodynamically, while *syn* is kinetically guided. Lower yield of the above-mentioned reaction performed at 0–5 °C, might be attributed to that initially kinetical *syn* product is formed, but its transformation to thermodynamical more stable *anti*-isomer is prevented at low temperature. Also, it is evident that chlorine presence, as electron withdrawing substituent in aniline, is accelerating reaction (**Method B**), and in that way, opens the door for the formation of *syn* product. Nevertheless, detailed mechanistic study of these reactions will be a subject of our further investigations.

Compared to the results of the other organocatalyzed reactions where products were obtained in moderate yields, **Method B** procedure provided products in good to excellent yields, with significantly shorter reaction time.[6,18,24,42] In addition, results presented here are comparable with reactions catalyzed with different, high performing metal based catalysts.[43–45] Furthermore, this report is the only supplement to the work of Mukhopadhyay at al. dealing with diastereoselectivity of MCRs for the synthesis of THPs up to now.[28]

Structural characterization

Newly synthesized THPs (**1**-**3**) were characterized based on IR, NMR (^{1}H, ^{13}C, and NOESY), and UV experimental and simulated spectral properties, as well as elemental analysis. For simulation of spectral properties and antioxidative mechanisms, the starting geometry of all examined compounds was based on the crystallographic structure of a similar compound obtained from the literature.[46] Firstly, optimizations were performed in gas phase to confirm the crystallographic structure, and so obtained structures were used for IR spectral characterization. Additionally, IR spectral properties were simulated in methanol and chloroform. To investigate NMR spectral properties, starting

points were generated from gas phase structures and fully optimized in chloroform, while for UV spectral properties as well as for mechanism of antioxidant action (parent molecule, radicals, anions, and radical cation) in methanol. It is worth pointing out, that selection of solvents for simulations was based on the solvents used in experiments. In addition, there is no significant structural difference between parent molecules optimized in gas phase, chloroform, and methanol.

IR spectral characterization

In the IR spectra of compounds **1–3** broad bands in the region of 3380–3550 cm^{-1} were attributed to the stretching vibrations of O–H groups, Figure 1. In all simulated spectra, these bands

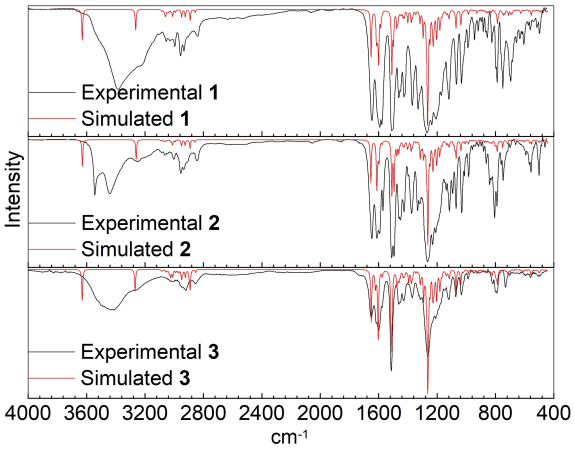

Figure 1. Experimental and simulated IR spectra of new THPs.

are significantly overestimated. This might be rationalized with intermolecular hydrogen bonding between two molecules of THP. Namely, although intramolecular hydrogen bonding was simulated between OH and adjacent OCH_3 groups on rings **C** and E (O–H…O–CH_3), interatomic distance in all vanillin based THPs between these groups is around 2.1 Å, implying week interaction. Additionally, experimental IR spectra were acquired in solid state (KBr pellet), while the simulated one in the gas phase. In contrast to this, excellent agreement between experimental and simulated N–H stretching vibrations (around 3250 cm^{-1}) was achieved. This confirmed presence of strong C=O…HN hydrogen bond. Furthermore, the bands in the region 2850–3050 cm^{-1} (both experimental and simulated) were attributed to the stretching vibrations of the aliphatic and aromatic CH, as well as aliphatic CH_2 and CH_3 groups in the molecules. The strong bands at 1650 cm^{-1} in all spectra were attributed to the stretching vibrations of carbonyl ester groups.

Vibration in the region 1580–1600 cm^{-1} originated from C=C stretching vibrations, while around 1550 and 1270 cm^{-1} from aromatic C=C bending and aliphatic C–N stretching vibrations, respectively. Comparison of the simulated spectra obtained using CPCM solvation model (methanol and chloroform solvents) and those obtained by gas phase calculations revealed that there is no crucial difference between them (Figures S1-S3).

NMR spectral characterization

In ^{1}H NMR spectra of compounds **1–3** (Tables S1 and S2), two methylene protons at **A5** (tetrahydropyridine ring labelled with **A** and carbon atom labelled with **5** in Scheme 1) appeared as two doublets of doublets at 2.67-2.74 ppm with coupling constants in range of 2.6-2.8 Hz (J_1) and 14.9-15.1 Hz (J_2), and at 2.89-2.91 with coupling constants in range of 5.1-5.4 Hz (J_1) and 14.7-15.0 Hz (J_2), respectively. The proton at chiral **A6** is represented by broad singlet around 5.00 ppm, while the one at **A2** is observed between 6.24-6.28 ppm together with aromatic protons. The aromatic protons appeared as multiplets and doublets in range of 6.20-7.10 ppm. The amino proton (NH) attached at **A4** appeared as broad singlet around 10.20 ppm. Methyl protons of two methoxy groups (substituents of rings **A** and **C**), and ester methoxy group appeared as singlets around 3.70, 3.80 and 3.90, respectively. In the case of compound **3**, two additional singlets originating from *p*-methyl groups of rings **B** and **D** appeared in the region of 2.16-2.30 ppm.

In ^{1}H NMR spectra of pure *syn* **11** product (obtained in mentioned "cold" conditions), two methylene protons at **A5** appeared as multiplets at 2.34–2.74 ppm. The proton at chiral **A6** is represented by doublet of doublets at 4.41–4.43 and 4.48–4.50 ppm with coupling constants of 3.7 Hz (J_1) and 12.3 Hz (J_2) while the one at **A2** is observed 5.94 ppm. The aromatic protons appeared as multiplets and doublets in range of 6.68–7.50 ppm. The amino proton (NH) attached at **A4** appeared as broad singlet around 10.59 ppm. Methyl proton of ester methoxy group appeared as singlet at 3.74 ppm.

Investigated compounds were characterized based on NOESY analysis, Figures 2 and S4. Inspection of these spectra

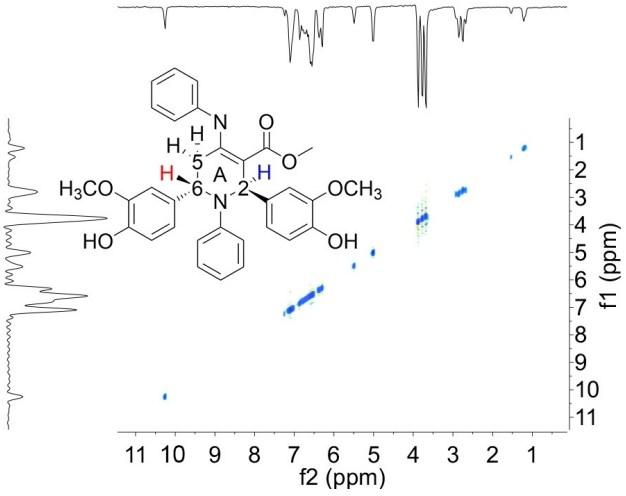

Figure 2. H–H NOESY spectrum of the compound **1.**

revealed that there is no interaction between **A2** and **A6** protons, clearly pointing out that these protons are exclusively oriented on the opposite sides of the plane of the ring **A**. Since this interaction is missing, it is obvious that these compounds are exclusively *anti* isomers. Additionally, there is no interaction between protons on neighboring **A5** and **A6** carbons, implying that these protons are also *anti*-oriented. This explains the appearance of broad singlet at around 5 ppm (**A6** proton) in place of doublet of doublets in ^{1}H NMR spectra of compounds **1–3**, as well as in all ^{1}H NMR spectra of other *anti*-products. On the other hand, NOESY spectrum of *syn* **11** (Figure S4) revealed that there is weak interaction between **A5** and **A6** protons, as well as weak interaction between **A2** and **A6** protons. This indicates that **A2** and **A6** protons are positioned on the same side of ring **A** plane.

To furtherly inspect the chemical shifts in experimental spectra, and to check whether obtained products are *anti* or *syn*, NMR spectra were simulated using Gauge-Independent Atomic Orbital (GIAO) method. Namely, simulated *anti* (Table S1) and *syn* chemical shifts (Table S2) were compared to the experimentally obtained values (Tables S1–3, Figure S5). Here, we point out that excellent agreement between all corresponding experimental and simulated spectra of *anti*-isomer was obtained, while detailed discussion is provided in Supporting Information.

UV-Vis spectral characterization

In addition to IR and NMR spectral characterization, UV–Vis spectra of the compounds subjected to this study are acquired and simulated, Figures 3, S8, and S9. In both, experimental and simulated spectra of compounds **1–3** there are three major absorption bands which appear in the regions around 250 nm, 290 nm, and 310 nm. The most significant deviation is in the case of **2**, where the experimental band at 262 nm is blue shifted to 253 nm in the simulated one. The experimental band of the same compound at 290 is red shifted to 299 nm in simulated. Average absolute error and average relative error amount 3.5 nm and 1.2%, Figure S10. To distinguish the parts of molecules responsible for electronic transitions, Kohn–Sham orbitals were constructed, Figures 3, S8, and S9. UV-Vis inspection revealed that HOMO-LUMO electron transition, as the lowest energy difference between the orbitals, is not responsible for the appearance of bands in UV-Vis spectra. This is caused by large spatial separation between these orbitals. Bands at shorter wavelengths of all investigated compounds are the consequence of electron transitions with large energy, but small spatial separation. On the other hand, bands around 290 and 310 nm are caused by transitions of relatively small energy gap. Detailed UV-Vis characterization is provided in Supporting information.

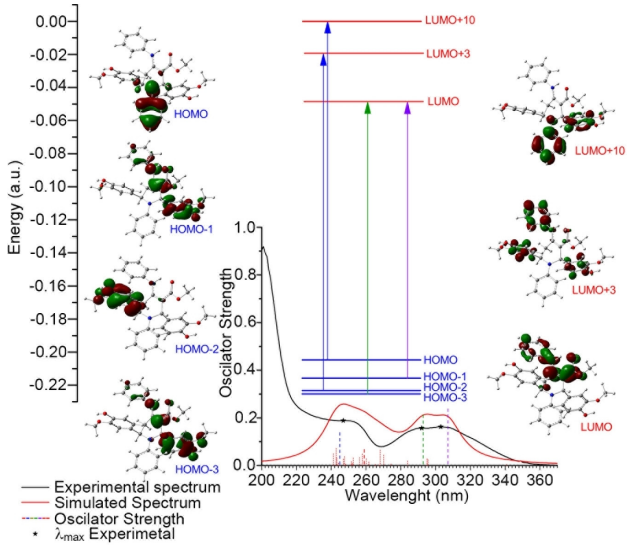

Figure 3. Experimental and simulated UV-Vis spectrum of **1** with delineated Kohn–Sham orbitals and electron transitions.

Antioxidative properties

DPPH test was used as experimental method for determining the antioxidant activity of newly obtained compounds.[47] It is known that this *in vitro* method is good in predicting antioxidant capacity towards reactive oxygen species present in the living cells.[48,49] The obtained results are presented in Table 4. Comparison of IC_{50} values of the control compound NDGA and of the investigated THPs revealed that they exerted somewhat lower activity. Taking into account activity of other compounds generally known as good antioxidants (phenolic acids, flavonols, isoflavones, flavanones, Schiff bases)[50–53] investigated THPs express significant antioxidant capacity, and can be considered as powerful radical scavengers.

Table 4. B3LYP/6-311 + G(d,p) calculated thermodynamical parameters of antioxidant mechanisms for all examined compounds in kJ mol-1

Compound	Radical source	HAT BDE	SET-PT IP	SET-PT PDE	SPLET PA	SPLET ETE	IC_{50} μM
	NH	377		106	201	340	
1	OH_C	324	436	53	172	317	9.0 ± 0.2
	OH_E	327		55	168	323	
	NH	377		99	195	346	
2	OH_C	325	442	47	170	319	13.1 ± 0.6
	OH_E	328		50	167	326	
	NH	373		117	206	332	
3	OH_C	324	421	67	172	316	8.6 ± 0.3
	OH_E	326		69	169	322	
NDGA							1.81 ± 0.1

In addition to the experimental determination of antioxidant activity, the most probable reaction pathway for radical scavenging activity, as well as free radical scavenging mechanisms of compounds **1**, **2** and **3** with different free radicals were determined from the thermodynamic point of view.

Table 5. Calculated reaction enthalpies (kJ mol^{-1}) for the reactions of the compound **1** with the selected radicals in methanol

	HAT ΔH_{BDE}			SET-PT ΔH_{IP}			ΔH_{PDE}			SPLET ΔH_{PA}			ΔH_{ETE}		
Radical/Compound	1	2	3	1	2	3	1	2	3	1	2	3	1	2	3
NH + •OH	-111	-111	-114				-130	-136	-119	-34	-41	-29	-77	-70	-85
OH_C + •OH	-164	-163	-164	19	25	5	-183	-188	-169	-64	-65	-63	-100	-98	-101
OH_E + •OH	-161	-160	-161				-180	-185	-166	-67	-69	-67	-94	-91	-95
NH + •OOH	27	27	24				-89	-95	-78	7	1	12	20	27	12
OH_C + •OOH	-26	-25	-26	116	123	102	-142	-147	-128	-23	-24	-22	-3	0	-4
OH_E + •OOH	-23	-22	-23				-139	-144	-125	-26	-28	-26	3	6	3
NH + CH_3OO•	37	37	33				-89	-96	-78	6	0	11	30	37	22
OH_C + CH_3OO•	-17	-15	-17	126	350	112	-142	-148	-128	-23	-25	-23	7	9	6
OH_E + CH_3OO•	-14	-13	-14				-140	-145	-126	-27	-28	-26	13	16	12
NH + •OO^-	111	111	108				-232	-239	-222	91	84	96	20	27	12
OH_C + •OO^-	58	59	58	344	132	329	-286	-291	-271	61	60	62	-3	0	-4
OH_E + •OO^-	61	62	61				-283	-288	-269	57	56	58	3	6	3
NH + CH_3O•	-40	-40	-44				-132	-139	-121	-36	-43	-32	-4	3	-12
OH_C + CH_3O•	-93	-92	-93	92	99	78	-185	-191	-171	-66	-68	-66	-27	-24	-28
OH_E + CH_3O•	-90	-89	-91				-183	-188	-169	-70	-71	-69	-20	-18	-21
NH + $(CH_3)_3C<C^->O$•	-47	-47	-50				-139	-145	-128	-43	-49	-38	-4	3	-12
OH_C + $(CH3)_3C<C^->O$•	-100	-99	-100	92	99	78	-192	-197	-178	-73	-74	-72	-27	-24	-28
OH_E + $(CH_3)_3C$–O•	-97	-96	-97				-189	-194	-175	-76	-78	-76	-21	-18	-21
NH + CH_2=CH–O–O•	36	36	32				-61	-67	-50	35	29	40	1	7	-8
OH_C + CH_2=CH–O–O•	-17	-16	-18	96	103	82	-114	-119	-100	5	4	6	-23	-20	-23
OH_E + CH_2=CH–O–O•	-15	-13	-15				-111	-116	-97	2	0	2	-16	-14	-17
NH + $_3$O–O•	2	2	-2				-11	-18	0	85	78	89	-83	-76	-91
OH_C + CCl_3O–O•	-51	-50	-51	13	20	-1	-64	-70	-50	55	53	55	-106	-103	-107
OH_E + CCl_3O–O•	-48	-47	-49				-62	-67	-47	51	50	52	-100	-97	-100

Antioxidative mechanisms of compound 1, 2, and 3

The most probable reaction pathway from the thermodynamic point of view can be determined by analysing the results presented in Table 4.[54–56] The preferred mechanism of antioxidant activity can be predicted from the BDE, IP, and PA values.[57,58] Detailed explanation of calculation of these parameters is provided in ESI. The lowest value is indicating the most possible mechanism. The values of PA are significantly lower from BDE and IP values for all investigated compounds, clearly showing that the SPLET is thermodynamically preferred mechanism. This finding is expected, since it is well known that heterolytic O–H bond cleavage is more probable than homolytic one in polar solvents.[59] Based on IP values of examined compounds, which are notably higher than those for BDEs and particularly PA values, it is obvious that SET-PT is not operative mechanism.

The first step of the SPLET mechanism is heterolytic cleavage of the O-H and N-H groups of compounds **1–3**, which leads to the formation of the corresponding anions. The stability of formed anions is consequence of the charge delocalisation, i.e. more delocalised charge contributes to higher stabilisation of anion. To get insight into this feature of THPs **1–3**, here we present absolute values of difference in natural charges between parent molecules and corresponding anions, Figures S11-S13. Based on this, it is clear that anions formed by deprotonation of the O–H bonds of the *para* phenolic groups are more stable than anion formed by heterolytic cleavage of N–H bond in all cases.

Although HAT is not the most probable mechanism of the reaction, radicals are formed in the final stage of SPLET mechanism, also. Therefore, stability of formed radicals influences the thermodynamic of the overall reaction, and has significant role in defining the antioxidant activity of the parent molecule. One of the ways to express this is via the spin density values of radicals. Namely, the stability of radical species increases with increase of delocalization of spin density. The values of these parameters for the compounds under investigation are presented in Figures S14-S16. Based on these values one can see that the radicals created from *p*-hydroxy groups are more stable than the one originating from N–H group. This is a consequence of delocalization of their unpaired electrons over the benzene ring, while the nitrogen originating one is delocalised mainly over adjacent double bond, with negligible contribution of neighbouring aromatic ring.

Free radical scavenging mechanisms of compound 1, 2, and 3 with different free radicals

The scavenging mechanisms are highly influenced by the electronic properties of the scavenged free radical species.[60] Bearing that in mind, the reaction enthalpies ($\Delta_r H$) of the compound **1, 2** and **3** with each of the eight selected free radicals (•OH, •OOH, CH_3–O–O•, O_2•$^-$, •OCH_3, •$OC(CH_3)_3$, CH_2=CH-O-O•, and Cl_3C-O-O•) were calculated for the above-mentioned mechanisms (HAT, SET-PT, and SPLET, Table 5).

Selected radicals are reactive oxygen species present in the organism, or they imitate behaviour of lipid peroxy radicals.[61] Superoxide radical anion (O_2•$^-$) is an important radical with

rather low reactivity. It is the product of single-electron reduction of oxygen. $O_2^{\bullet-}$ is formed as a product of respiration in living cells.[62] At pH lower than 4.8, superoxide can be protonated to give the more potent hydroperoxy radical (•OOH). In biological systems superoxide undergoes dismutation producing hydrogen peroxide (H_2O_2). Obtained hydrogen peroxide can suffer the Fenton and Haber-Weiss reactions, giving a powerful oxidant, the hydroxy radical (•OH).

Attack of •OH to hydrocarbons, in the presence of air, leads to the production of peroxy radicals, which are furtherly converted into the corresponding alkoxy radicals (for example $^{\bullet}OCH_3$ and $^{\bullet}OC(CH_3)_3$), via the reaction with NO.[63] The alkoxy radicals are much more harmful to the human body. The peroxy radicals •OOH, $CH_3OO^{\bullet}$, and $CH_2=CH\text{-}O\text{-}O^{\bullet}$ are less reactive than hydroxy and alkoxy radicals. On the other hand, $Cl_3COO^{\bullet}$ is very electronegative and highly reactive peroxy radical.

The obtained results for radical inactivation by studied compounds in methanol are presented in Table 5. The preferred mechanism can be assumed from the values of the basic processes: $\Delta_r H_{BDE}$, $\Delta_r H_{IP}$, and $\Delta_r H_{PA}$ values. More negative values indicate thermodynamically more possible mechanisms. This issue is presented in detail in ESI.

Based on values for $\Delta_r H_{IP}$ it is clear that SET-PT is not the operative scavenging mechanism in any case under investigation (Table 5), which is in agreement with thermodynamic results presented in Table 4. The negative or low positive values of $\Delta_r H_{BDE}$ and $\Delta_r H_{PA}$ indicate that in polar environment compounds **1–3** have a potential to scavenge all studied free radicals except $O_2^{\bullet-}$. The inactivation of $O_2^{\bullet-}$. with all examined compounds is not possible according to very endothermic processes. This is in accordance with the well-known fact that the $O_2^{\bullet-}$ is in equilibrium with •OOH.[64,65] The antiradical action of other radical species is represented with competition of HAT and SPLET mechanisms, which will be discussed in detail.

Inspection of the thermodynamic data for reactions of THPs **1–3** with •OH revealed that $\Delta_r H_{BDE}$ values are significantly lower than $\Delta_r H_{PA}$, specifying that HAT is preferred mechanism in this case, Table 5. Anyway, all examined compounds react with hydroxy radical very fast in all examined positions.[66] As expected, OH groups are more reactive than NH group.

The alkoxy radicals $^{\bullet}OCH_3$ and $^{\bullet}OC(CH_3)_3$ are highly reactive, but their reactions are less exothermic than those with •OH. Unlike the reactions with •OH, the difference between $\Delta_r H_{BDE}$ and $\Delta_r H_{PA}$ is not pronounced. Still, these parameters indicate that reaction with OH groups is faster than with NH, and that HAT mechanism is somewhat more favourable.

The values of reaction enthalpies of all investigated peroxy radicals are considerably higher than those for •OH and alkoxy radicals. This is in accordance with the fact that peroxy radicals are less reactive species than alkoxy radicals and •OH.[66] Analysis of data presented in Table 5 shows that HAT and SPLET are highly competitive mechanisms for the reactions with •OOH and $^{\bullet}OOCH_3$.

The thermodynamic data for reactions with $CH_2=CH\text{-}O\text{-}O^{\bullet}$ and $Cl_3COO^{\bullet}$ shows endothermic behaviour in the case of SPLET mechanism, Table 5. Since $\Delta_r H_{BDE}$ are expressing exothermic nature of the reaction, it can be assumed that HAT is probable mechanistic pathway in these cases. Based on the thermodynamic data for reactions of all peroxy radicals with NH group of investigated compounds, reaction in this position is not possible.

Conclusions

In this paper, we reported two novel, green, and diastereoselective protocols for the synthesis of THPs, using DHS as a catalyst and GA-promoted procedure. GA-promoted protocol proceeds faster and under mild reaction conditions, giving good to excellent yields (**Method B**). In addition, this protocol proceeds without costly and time-consuming purification processes, as well as without using toxic organic solvents. All these features point out this procedure as an elegant approach for the synthesis of highly functionalized THPs. Furthermore, the synthesis of three vanillic THPs **1–3** is reported here for the first time.

Newly obtained compounds were characterised using experimental and DFT tools (IR, NMR, and UV-Vis). Based on the ^{1}H NMR and NOESY spectra, as well as on simulated spectra, new compounds were characterized as *anti*-isomers.

Based on experimental and theoretical findings, the investigated THPs can be considered as powerful radical scavengers. Furthermore, thermodynamical parameters from Table 4 indicate SPLET as a favourable mechanism, while the results of radical inactivation (Table 5) indicate competition between HAT and SPLET mechanism, with favouring of HAT to some extent.

Supporting information Summary

All data regarding experimental section, details for calculations of thermodynamical parameters, thermodynamical parameters in the absence of free radical species, thermodynamic parameters in the presence of harmful free radicals, NMR spectral characterisation, Uv-Vis characterisation can be found in Supporting information.

Acknowledgements

This work was supported by the Ministry of Education, Science and Technological Development of the Republic of Serbia (projects No 172016, 174028). The authors are grateful to professor Svetlana Marković for useful suggestions.

Conflict of Interest

The authors declare no conflict of interest.

Keywords: Antioxidants · Density functional calculations · Multicomponent reactions · Structure elucidation · Synthetic methods

[1] V. Nair, C. Rajesh, A. U. Vinod, S. Bindu, A. R. Sreekanth, J. S. Mathen, L. Balagopal, *Acc. Chem. Res.* **2003**, *36*, 899–907.
[2] U. Christmann, R. Vilar, *Angew. Chemie - Int. Ed.* **2005**, *44*, 366–374.

[3] A. Dömling, *Chem. Rev.* **2006**, *106*, 17–89.
[4] T. Ahmadi, G. Mohammadi Ziarani, P. Gholamzadeh, H. Mollabagher, *Tetrahedron Asymmetry* **2017**, *28*, 708–724.
[5] B. B. Touré, D. G. Hall, *Chem. Rev.* **2009**, *109*, 4439–4486.
[6] A. T. Khan, M. Lal, M. M. Khan, *Tetrahedron Lett.* **2010**, *51*, 4419–4424.
[7] N. G. Kozlov, A. P. Kadutskii, *Tetrahedron Lett.* **2008**, *49*, 4560–4562.
[8] W. Zhu, M. Mena, E. Jnoff, N. Sun, P. Pasau, L. Ghosez, *Angew. Chemie Int. Ed.* **2009**, *48*, 5880–5883.
[9] A. M. Bender, N. W. Griggs, J. P. Anand, J. R. Traynor, E. M. Jutkiewicz, H. I. Mosberg, *ACS Chem. Neurosci.* **2015**, *6*, 1428–1435.
[10] J. Hou, W. Zhao, Z.-N. Huang, S.-M. Yang, L.-J. Wang, Y. Jiang, Z.-S. Zhou, M.-Y. Zheng, J.-L. Jiang, S.-H. Li, et al., *Chem. Biol. Drug Des.* **2014**, Epub ahead of print.
[11] S. Roslin, L. R. Odell, Y. Tsuji, Y. Watanabe, I. Ryu, T. Skrydstrup, I. Ryu, *Chem. Commun.* **2017**, *53*, 6895–6898.
[12] J. W. Bean, D. J. Nelson, G. E. Wright, *Biochem. Pharmacol.* **1986**, *35*, 1011–1017.
[13] N. Sharma, K. E. Carlson, J. C. Nwachukwu, S. Srinivasan, A. Sharma, K. W. Nettles, J. A. Katzenellenbogen, *ACS Chem. Biol.* **2017**, *12*, 494–503.
[14] J. W. Daly, T. F. Spande, H. M. Garraffo, *J. Nat. Prod.* **2005**, *68*, 1556–1575.
[15] D. O'Hagan, *Nat. Prod. Rep.* **2000**, *17*, 435–446.
[16] S. Petit, J. Nallet, M. Guillard, J. Dreux, R. Chermat, M. Poncelet, C. Bulach, P. Simon, C. Fontaine, M. Barthelmebs, et al., *Eur. J. Med. Chem.* **1991**, *26*, 19–32.
[17] Y. Zhou, V. E. Gregor, B. K. Ayida, G. C. Winters, Z. Sun, D. Murphy, G. Haley, D. Bailey, J. M. Froelich, S. Fish, et al., *Bioorganic Med. Chem. Lett.* **2007**, *17*, 1206–1210.
[18] M. Misra, S. K. Pandey, V. P. Pandey, J. Pandey, R. Tripathi, R. P. Tripathi, *Bioorganic Med. Chem.* **2009**, *17*, 625–633.
[19] B. Ho, A. Michael Crider, J. P. Stables, *Eur. J. Med. Chem.* **2001**, *36*, 265–286.
[20] A. F. Casy, R. B. Hussain, C. Upton, *Magn. Reson. Chem.* **1992**, *30*, 621–625.
[21] N. Sugiyama, F. Akahoshi, S. Kuwahara, M. Kajii, Y. Sakaue, H. Yakumaru, M. Sugiura, C. Fukaya, *J. Med. Chem.* **1994**, *37*, 1977–82.
[22] K. C. Nicolaou, B. S. Safina, M. Zak, A. A. Estrada, S. H. Lee, *Angew. Chemie - Int. Ed.* **2004**, *43*, 5087–5092.
[23] P. S. Watson, B. Jiang, B. Scott, *Org. Lett.* **2000**, *2*, 3679–3681.
[24] S. Verma, S. L. Jain, B. Sain, *Beilstein J. Org. Chem.* **2011**, *7*, 1334–1341.
[25] M. S. R. Murty, K. R. Ram, J. S. Yadav, *Tetrahedron Lett.* **2008**, *49*, 1141–1145.
[26] R. M. Carballo, M. A. Ramírez, M. L. Rodríguez, V. S. Martín, J. I. Padrón, *Org. Lett.* **2006**, *8*, 3837–3840.
[27] A. P. Dobbs, S. J. J. Guesné, *Synlett* **2005**, 2101–2103.
[28] C. Mukhopadhyay, S. Rana, R. J. Butcher, A. M. Schmiedekamp, *Tetrahedron Lett.* **2011**, *52*, 5835–5840.
[29] Z. D. Petrović, V. P. Petrović, D. Simijonović, S. Marković, *J. Mol. Catal. A Chem.* **2012**, *356*, 144–151.
[30] I. P. Beletskaya, A. V. Cheprakov, *Chem. Rev.* **2000**, *100*, 3009–3066.
[31] J. P. Hallett, T. Welton, *Chem. Rev.* **2011**, *111*, 3508–3576.
[32] T. Welton, *Chem. Rev.* **1999**, *99*, 2071–2083.
[33] V. P. Petrović, D. Simijonović, M. N. Živanović, J. V. Košarić, Z. D. Petrović, S. Marković, S. D. Marković, *RSC Adv.* **2014**, *4*, 24635–24644.
[34] M. Y. Lui, L. Crowhurst, J. P. Hallett, P. A. Hunt, H. Niedermeyer, T. Welton, *Chem. Sci.* **2011**, *2*, 1491.
[35] S. Zhang, K. Dokko, M. Watanabe, *Chem. Sci.* **2015**, *6*, 3684–3691.
[36] E. F. Bernstein, J. Lee, D. B. Brown, R. Yu, E. Van Scott, *Dermatol. Surg.* **2001**, *27*, 429–433.
[37] S.-C. Tang, P.-Y. Liao, S.-J. Hung, J.-S. Ge, S.-M. Chen, J.-C. Lai, Y.-P. Hsiao, J.-H. Yang, *J. Dermatol. Sci.* **2017**, *86*, 1–11.
[38] Y. Yamamoto, K. Uede, N. Yonei, A. Kishioka, T. Ohtani, F. Furukawa, *J. Dermatol.* **2006**, *33*, 16–22.
[39] X. S. Wu, *Artif. Cells, Blood Substitutes Biotechnol.* **2004**, *32*, 575–591.
[40] M. E. Alberto, N. Russo, A. Grand, A. Galano, *Phys. Chem. Chem. Phys.* **2013**, *15*, 4642.
[41] A. Galano, D. X. Tan, R. J. Reiter, *J. Pineal Res.* **2011**, *51*, 1–16.
[42] A. T. Khan, T. Parvin, L. H. Choudhury, *J. Org. Chem.* **2008**, *73*, 8398–8402.
[43] J. Safaei-ghomi, A. Ziarati, *Search Results J. Iran. Chem. Soc.* **2013**, 135–139.
[44] M. Kataria, S. Pramanik, M. Kumar, V. Bhalla, *Chem. Commun.* **2014**, *51*, 1483–1486.
[45] H. Eshghi, A. Khojastehnezhad, F. Moeinpour, S. Rezaeian, *Tetrahedron* **2015**, *71*, 436–444.
[46] M. M. Khan, S. Khan, S. Iqbal, S. Saigal, R. Yousuf, *New J. Chem.* **2016**, *40*, 7504–7512.
[47] C. Kontogiorgis, D. Hadjipavlou-Litina, *J. Enzyme Inhib. Med. Chem.* **2003**, *18*, 63–69.
[48] M. Miliovsky, I. Svinyarov, Y. Mitrev, Y. Evstatieva, D. Nikolova, M. Chochkova, M. G. Bogdanov, *Eur. J. Med. Chem.* **2013**, *66*, 185–192.
[49] S. Y. Li, X. B. Wang, L. Y. Kong, *Eur. J. Med. Chem.* **2014**, *71*, 36–45.
[50] Z. D. Petrović, J. Đorović, D. Simijonović, V. P. Petrović, Z. Marković, *RSC Adv.* **2015**, *5*, 24094–24100.
[51] Y.-Z. Cai, Mei Sun, Jie Xing, Q. Luo, H. Corke, *Life Sci.* **2006**, *78*, 2872–2888.
[52] J. Tošović, S. Marković, J. M. Dimitrić Marković, M. Mojović, D. Milenković, *Food Chem.* **2017**, *237*, 390–398.
[53] S. Marković, J. Tošović, *Food Chem.* **2016**, *210*, 585–592.
[54] A. Galano, G. Mazzone, R. Alvarez-Diduk, T. Marino, J. R. Alvarez-Idaboy, N. Russo, *Annu. Rev. Food Sci. Technol.* **2016**, *7*, 335–352.
[55] A. Galano, *J. Mex. Chem. Soc.* **2015**, *59*, 231–262.
[56] A. Pé rez-Gonzá lez, A. Galano, J. Raú Alvarez-Idaboy, *New J. Chem. New J. Chem* **2014**, *38*, 2639–2652.
[57] J. Rimarčík, V. Lukeš, E. Klein, M. Ilčin, *J. Mol. Struct. THEOCHEM* **2010**, *952*, 25–30.
[58] E. Klein, V. Lukeš, M. Ilčin, *Chem. Phys.* **2007**, *336*, 51–57.
[59] Z. Marković, D. Milenković, J. Đorović, J. M. Dimitrić Marković, V. Stepanić, B. Lučić, D. Amić, *Food Chem.* **2012**, *134*, 1754–1760.
[60] J. Xie, K. M. Schaich, *J. Agric. Food Chem.* **2014**, *62*, 4251–4260.
[61] A. Amić, Z. Marković, J. M. D. Marković, S. Jeremić, B. Lučić, D. Amić, *Comput. Biol. Chem.* **2016**, *65*, 45–53.
[62] H.-D. Belitz, W. Grosch, P. Schieberle, *Food Chemistry*, Springer Berlin Heidelberg, Berlin, Heidelberg, **2009**.
[63] J. J. Orlando, G. S. Tyndall, T. J. Wallington, *Chem. Rev.* **2003**, *103*, 4657–4689.
[64] X. Li, P. Fang, J. Mai, E. T. Choi, H. Wang, X. Yang, *J. Hematol. Oncol.* **2013**, *6*, 19.
[65] F. Muller, *J. Am. Aging Assoc.* **2000**, *23*, 227–253.
[66] J. Đorović, J. M. D. Marković, V. Stepanić, N. Begović, D. Amić, Z. Marković, *J. Mol. Model.* **2014**, *20*, 2345.

Submitted: August 16, 2017
Revised: November 22, 2017
Accepted: November 24, 2017